18th International Conference on Information Fusion
Washington, DC - July 6-9, 2015

Gaussian Mixture Multiple-Model Multi-Bernoulli Filters for Nonlinear Models Via Unscented Transforms

Tongyang Jiang*†, Meiqin Liu*†, Xie Wang†, and Senlin Zhang†
*State Key Laboratory of Industrial Control Technology, Zhejiang University, Hangzhou 310027, P.R. China
†College of Electrical Engineering, Zhejiang University, Hangzhou 310027, P.R. China
Email: {jiangtongyang,liumeiqin,wangxiek,slzhang}@zju.edu.cn

***Abstract*—The multiple-model multi-Bernoulli (MM-MB) filter is a new attractive approach for estimating multiple maneuvering targets in the presence of clutter, missed detection and data association uncertainty. In this paper, we extend the Gaussian Mixture (GM) MM-MB filter to nonlinear models by using unscented transform techniques. Moreover, in order to improve the robustness and numerical stability of the unscented Kalman (UK) GM-MM-MB filtering algorithm, we propose the square-root UK (SUK) GM implementation of the MM-MB filter for nonlinear models. A numerical example is presented to verify the effectiveness of the UK-GM-MM-MB and SUK-GM-MM-MB filtering approaches. Simulation results also show that the SUK-GM-MM-MB filtering approach produces the same filtering accuracy as the UK-GM-MM-MB filtering approach.**

I. Introduction

Random finite set (RFS) based multi-target tracking approaches have attracted more attention in recent years. The RFS-based approach treats the multi-target states and measurements as RFSs, and jointly estimates the number of targets and their states from the measurements. With RFS models, Mahler has proposed the optimal multi-target Bayes filter that propagates the posterior multi-target density recursively in time [1],[2]. However, since the optimal multi-target Bayes filter is generally intractable, some approximated approaches have been proposed, such as the probability hypothesis density (PHD) based on the first order moment approximation of multi-target density [1], the cardinalized PHD (CPHD) filter based on the moment and cardinality approximations [3], and multi-target multi-Bernoulli (MeMBer) filter based on density approximations [2]. Since the Mahler's MeMBer filter overestimates the number of target, Vo improved the MeMBer filter and proposed a new version of the MeMBer filter called the cardinality balanced (CB) MeMBer (CBMeMBer) filter which has an unbiased estimation in the number of targets [4]. The PHD, CPHD, and CBMeMBer filters have been implemented by using Gaussian mixture (GM) and sequential Monte Carlo (SMC) techniques [4],[5],[6],[7],[8]. In the SMC implementation, the CBMeMBer filter has a reliable and inexpensive extraction of target states, since it does not need an extra clustering algorithm for extracting target states [5]. In the GM implementation, the CBMeMBer filter shows the similar filtering performance to the PHD filter, and has a lower computation complexity than the CPHD filter [4]. The CBMeMber filter will be treated as the multi-Bernoulli (MB) filter throughout this paper.

For maneuvering target tracking, the multiple-model (MM) (or jump Markov system model) approach has proven to be an effective method [9]. By integrating the MB filter with MM approach, the MM-MB filter for maneuvering targets has been proposed in [10],[11]. The GM implementation of MM-MB filter for linear Gaussian models and the SMC implementation of MM-MB filter for nonlinear models were also proposed in [10],[11]. In target tracking, nonlinear models are commonly used, such as radar and sonar measurements are nonlinear [12]. Although the SMC-MM-MB filter can handle nonlinear models, it still has some disadvantages. Firstly, similar to the MM particle filter [13], the number of particles is proportional to the model probability, if the model probability is very low, only a small number of particles persists in the model. This may cause filtering divergence. Secondly, although the resampling step can reduce the degeneracy problem, it also causes the loss of diversity among the particles, as the particles after resampling step contain many repeated points. This phenomenon will be severe if the process noise is small. One solution to these problems is to increase the number of particles. However, a large number of particles means a large amount of calculation.

The GM-MM-MB filter has a close-form solution under assumptions of linear Gaussian models. However, the GM-MM-MB filter does not directly accommodate to nonlinear models. In addition, at present there is no closed form solution to GM-MM-MB filter for nonlinear models. Therefore, in this paper we extend the GM-MM-MB filter to nonlinear models by using unscented transforms [14]. Moreover, in order to improve the robustness and numerical stability of the unscented Kalman (UK) GM-MM-MB filter for nonlinear models, we propose the square-root UK (SUK) GM implementation of the MM-MB filter for nonlinear models. A numerical example is also presented to compare the UK-GM-MM-MB and SUK-GM-MM-MB filtering approach with the existing SMC-MM-MB filtering approach.

The rest of this paper is organized as follows. Section II provides the background on the MM-MB filter. The detailed description of the UK-GM-MM-MB and SUK-GM-MM-MB filtering approaches for nonlinear models are provided in

Section III. A numerical example is presented in Section IV. Finally, the conclusion is drawn in Section V.

II. The MM-MB Filter

The MM-MB filter has been proposed in [10],[11]. There is a little difference between [10] and [11]. In paper [11], the authors added an mixing stage before the predicted step. In this section we omit the mixing stage and adopt the MM-MB filter proposed by [10]. Here, we summarize the MM-MB filter as follows.

Prediction: If at time $k-1$, the posterior multi-target density

$$\pi_{k-1} = \{(r_{k-1}^{(i)}, p_{k-1}^{(i)}(x_{k-1}, s_{k-1}))\}_{i=1}^{M_{k-1}} \tag{1}$$

is given, where $r_{k-1}^{(i)}$ denotes the existence probability of the ith hypothesized track, $p_{k-1}^{(i)}(\cdot)$ denotes the probability density of the ith hypothesized track, M_{k-1} is the number of hypothesized tracks, s_{k-1} is the model variable at time $k-1$, then the predicted multi-target density is described by

$$\begin{aligned}\pi_{k|k-1} =& \{(r_{P,k|k-1}^{(i)}, p_{P,k|k-1}^{(i)}(x_k, s_k))\}_{i=1}^{M_{k-1}} \cup \\ & \{(r_{\Gamma,k}^{(i)}, p_{\Gamma,k}^{(i)}(x_k, s_k))\}_{i=1}^{M_{\Gamma,k}}\end{aligned} \tag{2}$$

where,

$$r_{P,k|k-1}^{(i)} = r_{k-1}^{(i)} \langle p_{k-1}^{(i)}(x_{k-1}, s_{k-1}), p_{S,k}(x_{k-1}, s_{k-1})\rangle \tag{3}$$

$$p_{P,k|k-1}^{(i)}(x_k, s_k) = \frac{\begin{array}{r}\big\langle f_{k|k-1}(x_k|x_{k-1}, s_k) t_{k|k-1}(s_k|s_{k-1}), \\ p_{k-1}^{(i)}(x_{k-1}, s_{k-1}) p_{S,k}(x_{k-1}, s_{k-1})\big\rangle\end{array}}{\big\langle p_{k-1}^{(i)}(x_{k-1}, s_{k-1}), p_{S,k}(x_{k-1}, s_k)\big\rangle} \tag{4}$$

$\langle\cdot,\cdot\rangle$ is the inner product defined between two real-valued functions α and β by $\langle\alpha,\beta\rangle = \int \alpha(x)\beta(x)dx$ (or $\sum_{i=0}^{\infty}\alpha(i)\beta(i)$, when α and β are sequences), $f_{k|k-1}(\cdot|x_{k-1}, s_k)$ denotes a single target transition density conditioned on model s_k, $t_{k|k-1}(\cdot|\cdot)$ is the motion transition probability, $p_{S,k}(x_k, s_k)$ is the existence probability of a target given state x_k conditioned on model s_k, and $\{(r_{\Gamma,k}^{(i)}, p_{\Gamma,k}^{(i)}(x_k, s_k))\}_{i=1}^{M_{\Gamma,k}}$ are the parameters of birth targets at time k.

Update: If at time k, the predicted multi-target density is

$$\pi_{k|k-1} = \{(r_{k|k-1}^{(i)}, p_{k|k-1}^{(i)}(x_k, s_k))\}_{i=1}^{M_{k|k-1}} \tag{5}$$

then the posterior multi-target density is approximated by

$$\begin{aligned}\pi_k =& \{(r_{L,k}^{(i)}, p_{L,k}^{(i)}(x_k, s_k))\}_{i=1}^{M_{k|k-1}} \cup \\ & \{(r_{U,k}(z_k), p_{U,k}(x_k, s_k; z_k))\}_{z_k \in Z_k}\end{aligned} \tag{6}$$

where

$$r_{L,k}^{(i)} = r_{k|k-1}^{(i)} \frac{1 - \big\langle p_{k|k-1}^{(i)}(x_k, s_k), p_{D,k}(x_k, s_k)\big\rangle}{1 - r_{k|k-1}^{(i)}\big\langle p_{k|k-1}^{(i)}(x_k, s_k), p_{D,k}(x_k, s_k)\big\rangle} \tag{7}$$

$$\begin{aligned}&p_{L,k}^{(i)}(x_k, s_k) = \\ &p_{k|k-1}^{(i)}(x_k, s_k)\frac{1 - p_{D,k}(x_k, s_k)}{1 - \big\langle p_{k|k-1}^{(i)}(x_k, s_k), p_{D,k}(x_k, s_k)\big\rangle}\end{aligned} \tag{8}$$

$$\begin{aligned}&r_{U,k}(z_k) = \\ &\frac{\sum_{i=1}^{M_{k|k-1}} \frac{r_{k|k-1}^{(i)}(1-r_{k|k-1}^{(i)})\langle p_{k|k-1}^{(i)}(x_k,s_k), \psi_{k,z}(x_k,s_k)\rangle}{(1-r_{k|k-1}^{(i)}\langle p_{k|k-1}^{(i)}(x_k,s_k), p_{D,k}(x_k,s_k)\rangle)^2}}{\kappa_k(z_k) + \sum_{i=1}^{M_{k|k-1}} \frac{r_{k|k-1}^{(i)}\langle p_{k|k-1}^{(i)}(x_k,s_k), \psi_{k,z}(x_k,s_k)\rangle}{1-r_{k|k-1}^{(i)}\langle p_{k|k-1}^{(i)}(x_k,s_k), p_{D,k}(x_k,s_k)\rangle}}\end{aligned} \tag{9}$$

$$\begin{aligned}&p_{U,k}(x_k, s_k; z_k) = \\ &\frac{\sum_{i=1}^{M_{k|k-1}} \frac{r_{k|k-1}^{(i)}}{1-r_{k|k-1}^{(i)}} p_{k|k-1}^{(i)}(x_k, s_k)\psi_{k,z}(x_k, s_k)}{\sum_{i=1}^{M_{k|k-1}} \frac{r_{k|k-1}^{(i)}}{1-r_{k|k-1}^{(i)}} \langle p_{k|k-1}^{(i)}(x_k, s_k), \psi_{k,z}(x_k, s_k)\rangle}\end{aligned} \tag{10}$$

$$\psi_{k,z}(x_k, s_k) = g_k(z_k|x_k, s_k) p_{D,k}(x_k, s_k) \tag{11}$$

where Z_k is the measurement set at time k, $g_k(\cdot|x_k, s_k)$ is the single measurement likelihood given state x_k conditioned on model s_k at time k, $p_{D,k}(x_k, s_k)$ is the detection probability conditioned on model s_k at time k, and $\kappa_k(\cdot)$ is the clutter intensity at time k.

From the recursive equations of the MM-MB filter, we can see that the MM-MB filter is similar to the MB filter. The key idea of the MM-MB filter is that the model variable is augmented for the recursions of the MB filter.

III. The GM-MM-MB Filter for Nonlinear Models

Although the GM-MM-MB filter has a closed form solution for linear Gaussian models, it does not accommodate to nonlinear models. In single target tracking, the UK filter is an attractive approach for nonlinear filtering [14]. Hence, in this section we propose the GM-MM-MB filter for nonlinear models by using unscented transform techniques.

A. The UK-GM-MM-MB Filtering Approach

Suppose the motion and measurement model of each target for a given model are nonlinear, which are described by

$$x_k = f_k(x_{k-1}, s_k) + w_{k-1}(s_k) \tag{12}$$

$$z_k = h_k(x_k, s_k) + v_k(s_k) \tag{13}$$

where $f_k(\cdot)$ and $h_k(\cdot)$ are the known nonlinear functions, $w_{k-1}(s_k)$ and $v_k(s_k)$ are independent zero mean Gaussian process noise and measurement noise with known covariances $Q_{k-1}(s_k)$ and $R_k(s_k)$, respectively. The survival probability and detection probability are assumed to be state independent, i.e. $p_{S,k}(x_{k-1}, s_{k-1}) = p_{S,k}(s_{k-1})$, $p_{D,k}(x_k, s_k) = p_{D,k}(s_k)$. Based on the unscented transform techniques and the GM-MM-MB filter, the UK-GM-MM-MB filtering approach can be obtained.

Prediction: If at time $k-1$, the posterior multi-target density is given by (1), and each probability density $p_{k-1}^{(i)}(x_{k-1}, s_{k-1})$ is the form of GM, i.e.

$$\begin{aligned}&p_{k-1}^{(i)}(x_{k-1}, s_{k-1}) = \\ &\sum_{j=1}^{J_{k-1}^{(i)}(s_{k-1})} w_{k-1}^{(i,j)}(s_{k-1})\mathcal{N}(x_{k-1}; m_{k-1}^{(i,j)}(s_{k-1}), P_{k-1}^{(i,j)}(s_{k-1}))\end{aligned} \tag{14}$$

then the predicted multi-target density (2) can be computed as follows:

$$r_{P,k|k-1}^{(i)} = r_{k-1}^{(i)} \sum_{s_{k-1}} \sum_{j=1}^{J_{k-1}^{(i)}(s_{k-1})} w_{k-1}^{(i,j)}(s_{k-1}) p_{S,k}(s_{k-1}), \tag{15}$$

$$p_{P,k|k-1}^{(i)}(x_k, s_k) = \sum_{s_{k-1}} \sum_{j=1}^{J_{k-1}^{(i)}(s_{k-1})} w_{P,k|k-1}^{(i,j)}(s_k, s_{k-1}) \times \mathcal{N}(x_k; m_{P,k|k-1}^{(i,j)}(s_k, s_{k-1}), P_{P,k|k-1}^{(i,j)}(s_k, s_{k-1})) \tag{16}$$

where

$$\chi_{k-1}^{(i,j)}(s_{k-1}) = \Big[m_{k-1}^{(i,j)}(s_{k-1}) \quad m_{k-1}^{(i,j)}(s_{k-1}) + \gamma \big[B_{k-1}^{(i,j)}(s_{k-1}) \big]_l \quad m_{k-1}^{(i,j)}(s_{k-1}) - \gamma \big[B_{k-1}^{(i,j)}(s_{k-1}) \big]_l \Big], l = 1, \cdots, n \tag{17}$$

$$\gamma = \sqrt{n + \lambda} \tag{18}$$

$$P_{k-1}^{(i,j)}(s_{k-1}) = B_{k-1}^{(i,j)}(s_{k-1}) (B_{k-1}^{(i,j)}(s_{k-1}))^T \tag{19}$$

$$\mathcal{X}_{l,k|k-1}^{(i,j)}(s_k, s_{k-1}) = f_k(\chi_{l,k-1}^{(i,j)}(s_{k-1}), s_k), l = 0, \cdots, 2n \tag{20}$$

$$m_{P,k|k-1}^{(i,j)}(s_k, s_{k-1}) = \sum_{l=0}^{2n} W^a(l) \mathcal{X}_{l,k|k-1}^{(i,j)}(s_k, s_{k-1}) \tag{21}$$

$$w_{P,k|k-1}^{(i,j)}(s_k, s_{k-1}) = \frac{w_{k-1}^{(i,j)}(s_{k-1}) p_{S,k}(s_{k-1}) t_{k|k-1}(s_k | s_{k-1})}{\sum_{s_{k-1}} \sum_{j=1}^{J_{k-1}^{(i)}(s_{k-1})} w_{k-1}^{(i,j)}(s_{k-1}) p_{S,k}(s_{k-1})} \tag{22}$$

$$P_{P,k|k-1}^{(i,j)}(s_k, s_{k-1}) = \sum_{l=0}^{2n} W^c(l) (m_{P,k|k-1}^{(i,j)}(s_k, s_{k-1}) - \mathcal{X}_{l,k|k-1}^{(i,j)}(s_k, s_{k-1})) \times (m_{P,k|k-1}^{(i,j)}(s_k, s_{k-1}) - \mathcal{X}_{l,k|k-1}^{(i,j)}(s_k, s_{k-1}))^T + Q_{k-1}(s_k) \tag{23}$$

$$W^a = \left[\frac{\lambda}{(n+\lambda)}, \underbrace{\frac{1}{2(n+\lambda)}, \cdots, \frac{1}{2(n+\lambda)}}_{2n} \right] \tag{24}$$

$$W^c = \left[\frac{\lambda}{(n+\lambda)} + (1 - \alpha^2 + \beta), \underbrace{\frac{1}{2(n+\lambda)}, \cdots, \frac{1}{2(n+\lambda)}}_{2n} \right] \tag{25}$$

n is the dimension of the state $m_{k-1}^{(i,j)}(s_{k-1})$, λ, α, and β are the scaling parameters [15], and $[\cdot]_l$ denotes the lth column of the matrix. $\{(r_{\Gamma,k}^{(i)}, p_{\Gamma,k}^{(i)}(x_k, s_k))\}_{i=1}^{M_{\Gamma,k}}$ are parameters of birth targets, and $p_{\Gamma,k}^{(i)}(x_k, s_k)$ is given by

$$p_{\Gamma,k}^{(i)}(x_k, s_k) = t_{\Gamma,k}^{(i)}(s_k) \sum_{j=1}^{J_{\Gamma,k}^{(i)}(s_k)} w_{\Gamma,k}^{(i,j)}(s_k) \mathcal{N}(x_k; m_{\Gamma,k}^{(i,j)}(s_k), P_{\Gamma,k}^{(i,j)}(s_k)) \tag{26}$$

$t_{\Gamma,k}^{(i)}(\cdot)$ is the probability distribution of the models for given birth targets, and $w_{\Gamma,k}^{(i,j)}(\cdot)$, $m_{\Gamma,k}^{(i,j)}(\cdot)$, $P_{\Gamma,k}^{(i,j)}(\cdot)$ are given parameters.

Update: If at time k, the predicted multi-target density (5) is given and each probability $p_{k|k-1}^{(i)}(x_k, s_k)$ is the form of GM, i.e.

$$p_{k|k-1}^{(i)}(x_k, s_k) = \sum_{j=1}^{J_{k|k-1}^{(i)}(s_k)} w_{k|k-1}^{(i,j)}(s_k) \mathcal{N}(x_k; m_{k|k-1}^{(i,j)}(s_k), P_{k|k-1}^{(i,j)}(s_k)), \tag{27}$$

then the updated density (6) can be computed as follows:

The legacy track components are

$$r_{L,k}^{(i)} = r_{k|k-1}^{(i)} \frac{1 - \varrho_{L,k}^{(i)}}{1 - r_{k|k-1}^{(i)} \varrho_{L,k}^{(i)}} \tag{28}$$

$$p_{L,k}^{(i)}(x_k, s_k) = \sum_{j=1}^{J_{k|k-1}^{(i)}(s_k)} w_{L,k}^{(i,j)}(s_k) \mathcal{N}(x_k; m_{k|k-1}^{(i,j)}(s_k), P_{k|k-1}^{(i,j)}(s_k)) \tag{29}$$

where

$$\varrho_{L,k}^{(i)} = \sum_{s_k} \sum_{j=1}^{J_{k|k-1}^{(i)}(s_k)} w_{k|k-1}^{(i,j)}(s_k) p_{D,k}(s_k) \tag{30}$$

$$w_{L,k}^{(i,j)}(s_k) = \frac{w_{k|k-1}^{(i,j)}(s_k)(1 - p_{D,k}(s_k))}{1 - \varrho_{L,k}^{(i)}} \tag{31}$$

The measurement-updated track components are

$$r_{U,k}(z_k) = \frac{\sum_{i=1}^{M_{k|k-1}} \frac{r_{k|k-1}^{(i)}(1 - r_{k|k-1}^{(i)}) \varrho_{U,k}^{(i)}(z_k)}{(1 - r_{k|k-1}^{(i)} \varrho_{L,k}^{(i)})^2}}{\kappa_k(z_k) + \sum_{i=1}^{M_{k|k-1}} \frac{r_{k|k-1}^{(i)} \varrho_{U,k}^{(i)}(z_k)}{1 - r_{k|k-1}^{(i)} \varrho_{L,k}^{(i)}}} \tag{32}$$

$$p_{U,k}(x_k, s_k; z_k) = \sum_{i=1}^{M_{k|k-1}} \sum_{j=1}^{J_{k|k-1}^{(i)}(s_k)} w_{U,k}^{(i,j)}(s_k; z_k) \times \mathcal{N}(x_k, m_{U,k}^{(i,j)}(s_k; z_k), P_{U,k}^{(i,j)}(s_k; z_k)) \tag{33}$$

where

$$\varrho_{U,k}^{(i)}(z_k) = \sum_{s_k} \sum_{j=1}^{J_{k|k-1}^{(i)}(s_k)} w_{k|k-1}^{(i,j)}(s_k) p_{D,k}(s_k) q_k^{(i,j)}(s_k; z_k) \tag{34}$$

$$\chi_{k|k-1}^{(i,j)}(s_k) = \Big[m_{k|k-1}^{(i,j)}(s_k) \quad m_{k|k-1}^{(i,j)}(s_k) + \gamma \big[B_{k|k-1}^{(i,j)}(s_k) \big]_l \quad m_{k|k-1}^{(i,j)}(s_k) - \gamma \big[B_{k|k-1}^{(i,j)}(s_k) \big]_l \Big], l = 1, \cdots, n \tag{35}$$

$$P_{k|k-1}^{(i,j)}(s_k) = B_{k|k-1}^{(i,j)}(s_k) (B_{k|k-1}^{(i,j)}(s_k))^T \tag{36}$$

$$z_{l,k|k-1}^{(i,j)}(s_k) = h_k(\chi_{l,k|k-1}^{(i,j)}(s_k), s_k), l = 0, 1, \cdots, 2n \tag{37}$$

$$\eta^{(i,j)}_{U,k|k-1}(s_k) = \sum_{l=0}^{2n} W^a(l) z^{(i,j)}_{l,k|k-1}(s_k) \tag{38}$$

$$q^{(i,j)}_k(s_k; z_k) = \mathcal{N}(z_k; \eta^{(i,j)}_{U,k|k-1}(s_k), S^{(i,j)}_{U,k}(s_k)) \tag{39}$$

$$S^{(i,j)}_{U,k}(s_k) = \sum_{l=0}^{2n} W^c(l)(\eta^{(i,j)}_{U,k|k-1}(s_k) - z^{(i,j)}_{l,k|k-1}(s_k))\times (\eta^{(i,j)}_{U,k|k-1}(s_k) - z^{(i,j)}_{l,k|k-1}(s_k))^T + R_k(s_k) \tag{40}$$

$$G^{(i,j)}_{U,k}(s_k) = \sum_{l=0}^{2n} W^c(l)(m^{(i,j)}_{k|k-1} - \chi^{(i,j)}_{l,k|k-1}(s_k))\times (\eta^{(i,j)}_{U,k|k-1}(s_k) - z^{(i,j)}_{l,k|k-1}(s_k))^T \tag{41}$$

$$K^{(i,j)}_{U,k}(s_k) = G^{(i,j)}_{U,k}(s_k)\left[S^{(i,j)}_{U,k}(s_k)\right]^{-1} \tag{42}$$

$$w^{(i,j)}_{U,k}(s_k; z_k) = \frac{\frac{r^{(i)}_{k|k-1}}{1-r^{(i)}_{k|k-1}} w^{(i,j)}_{k|k-1}(s_k) q^{(i,j)}_k(s_k; z_k) p_{D,k}(s_k)}{\sum_{i=1}^{M_{k|k-1}} \frac{r^{(i)}_{k|k-1}}{1-r^{(i)}_{k|k-1}} \varrho^{(i)}_{U,k}(z_k)} \tag{43}$$

$$m^{(i,j)}_{U,k}(s_k; z_k) = m^{(i,j)}_{k|k-1}(s_k) + K^{(i,j)}_{U,k}(s_k)(z_k - \eta^{(i,j)}_{U,k|k-1}(s_k)) \tag{44}$$

$$P^{(i,j)}_{U,k}(s_k; z_k) = P^{(i,j)}_{k|k-1}(s_k) - K^{(i,j)}_{U,k}(s_k) S^{(i,j)}_{U,k}(s_k)(K^{(i,j)}_{U,k}(s_k))^T \tag{45}$$

Multi-target state extraction: extract multi-target states is the same as that of the GM-MM-MB filter, for more details see [10].

B. The SUK-GM-MM-MB Filtering Approach

From the UK-GM-MM-MB filter recursions, we can see that while designing the sigma points for each hypothesized track, we should compute the square-root of state covariance matrices. Hence the state covariance matrices should be positive definite. However, due to the error caused by the arithmetic operation performed on digital computers, the state covariance matrixes may not be positive definite. This phenomenon may cause numerical problems. To improve the robustness and numerical stability, inspired by [16] we propose the SUK-GM implementation of the MM-MB filter for nonlinear models. While propagating the MB parameters, the SUK-GM-MM-MB filtering approach directly propagates square-root of the state covariances. So this can avoid the square-rooting operations. The SUK-GM-MM-MB filtering approach is given as follows.

Prediction: If at time $k-1$, the posterior multi-target density is given by (1), and each probability density $p^{(i)}_{k-1}(x_{k-1}, s_{k-1})$ is described by

$$p^{(i)}_{k-1}(x_{k-1}, s_{k-1}) = \sum_{j=1}^{J^{(i)}_{k-1}(s_{k-1})} w^{(i,j)}_{k-1}(s_{k-1}) \mathcal{N}(x_{k-1}; m^{(i,j)}_{k-1}(s_{k-1}), C^{(i,j)}_{k-1}(s_{k-1})(C^{(i,j)}_{k-1}(s_{k-1}))^T) \tag{46}$$

then the predicted multi-target density (2) can be computed as follows: compute $r^{(i)}_{P,k|k-1}$ according to (15)

$$p^{(i)}_{P,k|k-1}(x_k, s_k) = \sum_{s_{k-1}} \sum_{j=1}^{J^{(i)}_{k-1}(s_{k-1})} w^{(i,j)}_{P,k|k-1}(s_k, s_{k-1})\times \mathcal{N}(x_k; m^{(i,j)}_{P,k|k-1}(s_k, s_{k-1}), C^{(i,j)}_{P,k|k-1}(s_k, s_{k-1})(C^{(i,j)}_{P,k|k-1}(s_k, s_{k-1}))^T) \tag{47}$$

$$\chi^{(i,j)}_{k-1}(s_{k-1}) = \Big[m^{(i,j)}_{k-1}(s_{k-1}) \;\; m^{(i,j)}_{k-1}(s_{k-1}) + \gamma\big[C^{(i,j)}_{k-1}(s_{k-1})\big]_l \;\; m^{(i,j)}_{k-1}(s_{k-1}) - \gamma\big[C^{(i,j)}_{k-1}(s_{k-1})\big]_l\Big], l = 1, \cdots, n \tag{48}$$

compute γ, $\mathcal{X}^{(i,j)}_{l,k|k-1}(s_k, s_{k-1})$, $m^{(i,j)}_{P,k|k-1}(s_k, s_{k-1})$, and $w^{(i,j)}_{P,k|k-1}(s_k, s_{k-1})$ according to (18), (20), (21) and (22), respectively.

$$\mathcal{X}^{*(i,j)}_{k|k-1}(s_k, s_{k-1}) = \Big[\sqrt{W^c(0)}\big(\mathcal{X}^{(i,j)}_{0,k|k-1}(s_k, s_{k-1}) - m^{(i,j)}_{P,k|k-1}(s_k, s_{k-1})\big), \sqrt{W^c(1)}\big(\mathcal{X}^{(i,j)}_{1,k|k-1}(s_k, s_{k-1}) - m^{(i,j)}_{P,k|k-1}(s_k, s_{k-1})\big), \cdots, \sqrt{W^c(2n)}\big(\mathcal{X}^{(i,j)}_{2n,k|k-1}(s_k, s_{k-1}) - m^{(i,j)}_{P,k|k-1}(s_k, s_{k-1})\big)\Big] \tag{49}$$

$$C^{(i,j)}_{P,k|k-1}(s_k, s_{k-1}) = \textbf{Tria}([\mathcal{X}^{*(i,j)}_{k|k-1}(s_k, s_{k-1}), C_{Q,k-1}(s_{k-1})]) \tag{50}$$

$$Q_{k-1}(s_{k-1}) = C_{Q,k-1}(s_{k-1})(C_{Q,k-1}(s_{k-1}))^T \tag{51}$$

"**Tria**" denotes a general triangularization algorithm. For example, $S = \textbf{Tria}(A)$, where S is the lower triangular matrix. Let R be an upper triangular matrix obtained from QR decomposition on A^T, then $S = R^T$ [17].

Update: If at time k, the predicted multi-target density (5) is given, and each probability $p^{(i)}_{k|k-1}(x_k, s_k)$ is described by

$$p^{(i)}_{k|k-1}(x_k, s_k) = \sum_{j=1}^{J^{(i)}_{k|k-1}(s_k)} w^{(i,j)}_{k|k-1}(s_k) \mathcal{N}(x_k; m^{(i,j)}_{k|k-1}(s_k), C^{(i,j)}_{k|k-1}(s_k)(C^{(i,j)}_{k|k-1}(s_k))^T), \tag{52}$$

then the updated density (6) can be computed as follows:

The legacy track components: compute $\varrho^{(i)}_{L,k}$ and $r^{(i)}_{L,k}$ according to (30) and (28), respectively.

$$p^{(i)}_{L,k}(x_k, s_k) = \sum_{j=1}^{J^{(i)}_{k|k-1}(s_k)} w^{(i,j)}_{L,k}(s_k) \mathcal{N}(x_k; m^{(i,j)}_{k|k-1}(s_k), C^{(i,j)}_{k|k-1}(s_k)(C^{(i,j)}_{k|k-1}(s_k))^T) \tag{53}$$

The measurement-updated track components: compute

$r_{U,k}(z_k)$ according to (32)

$$p_{U,k}(x_k, s_k; z_k) = \sum_{i=1}^{M_{k|k-1}} \sum_{j=1}^{J_{k|k-1}^{(i)}(s_k)} w_{U,k}^{(i,j)}(s_k; z_k) \times \mathcal{N}(x_k, m_{U,k}^{(i,j)}(s_k; z_k), C_{U,k}^{(i,j)}(s_k; z_k)(C_{U,k}^{(i,j)}(s_k; z_k))^T) \tag{54}$$

where

$$\chi_{k|k-1}^{(i,j)}(s_k) = \Big[m_{k|k-1}^{(i,j)}(s_k) \quad m_{k|k-1}^{(i,j)}(s_k) + \gamma[C_{k|k-1}^{(i,j)}(s_k)]_l \quad m_{k-1}^{(i,j)}(s_{k-1}) - \gamma[C_{k|k-1}^{(i,j)}(s_k)]_l\Big], l = 1, \cdots, n \tag{55}$$

$\varrho_{U,k}^{(i)}(z_k)$, $z_{l,k|k-1}^{(i,j)}(s_k)$ and $\eta_{U,k|k-1}^{(i,j)}(s_k)$ are computed according to (34),(37) and (38), respectively.

$$\mathcal{Z}_{U,k|k-1}^{(i,j)}(s_k) = \Big[\sqrt{W^c(0)}\big(z_{0,k|k-1}^{(i,j)}(s_k) - \eta_{U,k|k-1}^{(i,j)}(s_k)\big), \sqrt{W^c(1)}\big(z_{1,k|k-1}^{(i,j)}(s_k) - \eta_{U,k|k-1}^{(i,j)}(s_k)\big), \cdots, \sqrt{W^c(2n)}\big(z_{2n,k|k-1}^{(i,j)}(s_k) - \eta_{U,k|k-1}^{(i,j)}(s_k)\big)\Big] \tag{56}$$

$$\mathcal{X}_{U,k|k-1}^{(i,j)}(s_k) = \Big[\sqrt{W^c(0)}\big(\chi_{0,k|k-1}^{(i,j)}(s_k) - m_{k|k-1}^{(i,j)}(s_k)\big), \sqrt{W^c(1)}\big(\chi_{1,k|k-1}^{(i,j)}(s_k) - m_{k|k-1}^{(i,j)}(s_k)\big), \cdots, \sqrt{W^c(2n)}\big(\chi_{2n,k|k-1}^{(i,j)}(s_k) - m_{k|k-1}^{(i,j)}(s_k)\big)\Big] \tag{57}$$

$$C_{zz,k|k-1}(s_k) = \textbf{Tria}([\mathcal{Z}_{U,k|k-1}^{(i,j)}(s_k), C_{R,k}(s_k)]) \tag{58}$$

$$R_k(s_k) = C_{R,k}(s_k)(C_{R,k}(s_k))^T \tag{59}$$

$$S_{U,k}^{(i,j)}(s_k) = \mathcal{Z}_{U,k|k-1}^{(i,j)}(s_k)(\mathcal{Z}_{U,k|k-1}^{(i,j)}(s_k))^T \tag{60}$$

$$G_{U,k}^{(i,j)}(s_k) = \mathcal{X}_{U,k|k-1}^{(i,j)}(s_k)(\mathcal{Z}_{U,k|k-1}^{(i,j)}(s_k))^T \tag{61}$$

$$K_{U,k}^{(i,j)}(s_k) = (G_{U,k}^{(i,j)}(s_k)/(C_{zz,k|k-1}(s_k))^T)/C_{zz,k|k-1}(s_k) \tag{62}$$

$q_k^{(i,j)}(s_k; z_k)$, $w_{U,k}^{(i,j)}(s_k; z_k)$, $m_{U,k}^{(i,j)}(s_k; z_k)$ are computed according to (39), (43), and (44), respectively.

$$C_{U,k}^{(i,j)}(s_k; z_k) = \textbf{Tria}([\mathcal{X}_{U,k|k-1}^{(i,j)}(s_k) - K_{U,k}^{(i,j)}(s_k) \times \mathcal{Z}_{U,k|k-1}^{(i,j)}(s_k), K_{U,k}^{(i,j)}(s_k)C_{R,k}(s_k)]) \tag{63}$$

From the above recursions we can see that, the SUK-GM-MM-MB filtering approach directly propagates the square-root of state covariances. So square-rooting operations are avoided. This improves the robustness and numerical stability of the UK-GM-MM-MB filtering approach.

IV. Simulation Results

A. Simulation Scenario

Consider the noisy bearings and range measurements with varying number of targets observed in clutter and missed detection environments. The surveillance region size is $[0, \pi]$ rad $\times$ $[0, 2000]$ m. A maximum of 10 maneuvering targets appears in the scenario, and targets appear and terminate at a random time. The true target tracks are shown in Fig. 2. The kinematic state of the target $x_k = [p_{x,k}, \dot{p}_{x,k}, p_{y,k}, \dot{p}_{y,k}, \omega_k]^T$ consists of the position $(p_{x,k}, p_{y,k})$, velocity $(\dot{p}_{x,k}, \dot{p}_{y,k})$, and turn rate ω_k. For the coordinated turn (CT) model, if the turn rate is not a constant, the CT model becomes a nonlinear one. The CT model is described by [18]

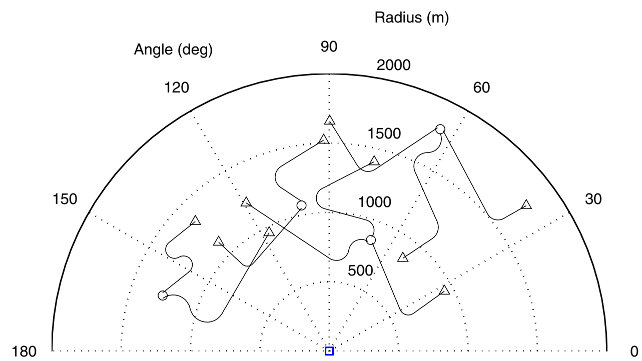

Fig. 1. True target tracks in $r\theta$ plane (the start/end positions for each track are denoted by $\circ/\triangle$, and the sensor is denoted by $\square$).

$$x_k = F(\omega_{k-1})x_{k-1} + w_{k-1}, \tag{64}$$

The process noise $w_{k-1} \sim \mathcal{N}(\cdot; 0, Q_{k-1})$, and the matrices $F(\omega_{k-1})$ and Q_{k-1} are given as follows

$$F(\omega_{k-1}) = \begin{bmatrix} 1 & \frac{\sin\omega_{k-1}T}{\omega_{k-1}} & 0 & -\frac{1-\cos\omega_{k-1}T}{\omega_{k-1}} & 0 \\ 0 & \cos\omega_{k-1}T & 0 & -\sin\omega_{k-1}T & 0 \\ 0 & \frac{1-\cos\omega_{k-1}T}{\omega_{k-1}} & 1 & \frac{\sin\omega_{k-1}T}{\omega_{k-1}} & 0 \\ 0 & \sin\omega_{k-1}T & 0 & \cos\omega_{k-1}T & 0 \\ 0 & 0 & 0 & 0 & 1 \end{bmatrix}, \tag{65}$$

$$Q_{k-1} = \begin{bmatrix} \frac{T^3}{3}\tilde{q}_w & \frac{T^2}{2}\tilde{q}_w & 0 & 0 & 0 \\ \frac{T^2}{2}\tilde{q}_w & T\tilde{q}_w & 0 & 0 & 0 \\ 0 & 0 & \frac{T^3}{3}\tilde{q}_w & \frac{T^2}{2}\tilde{q}_w & 0 \\ 0 & 0 & \frac{T^2}{2}\tilde{q}_w & T\tilde{q}_w & 0 \\ 0 & 0 & 0 & 0 & T\tilde{q}_\omega \end{bmatrix} \tag{66}$$

where $\tilde{q}_w$ and $\tilde{q}_\omega$ are related to the process noise intensities. $T = 1$ s is the sampling period.

Two motion models are used: Model 1 is a CT model with a known turn rate of 0 rad/s. Model 2 is a CT model with an unknown turn rate. The standard deviations of the process are $\tilde{q}_w = 0.25$ m^2/s^3 and $\tilde{q}_\omega = 0.04$ rad^2/s^3 for motion 1 and model 2. The transition probability matrix is set to

$$t_{k|k-1}(s_k|s_{k-1}) = \begin{bmatrix} 0.6 & 0.4 \\ 0.4 & 0.6 \end{bmatrix}, \tag{67}$$

The measurement is the noisy bearing and range model [6], which is described by

$$z_k = \begin{bmatrix} \arctan\left(\frac{p_{x,k} - p_{\mathrm{Se},x}}{p_{y,k} - p_{\mathrm{Se},y}}\right) \\ \sqrt{(p_{x,k} - p_{\mathrm{Se},x})^2 + (p_{y,k} - p_{\mathrm{Se},y})^2} \end{bmatrix} + v_k, \tag{68}$$

where $(p_{\mathrm{Se},x}, p_{\mathrm{Se},y}) = (0, 0)$ m is the position of the sensor, The measurement noise v_k follows a zero mean Gaussian distribution with the known covariance $R_k = \mathrm{diag}\{\sigma_\theta, \sigma_r\}^2$, where $\sigma_\theta = 1 \times (\pi/180)$ rad and $\sigma_r = 5$ m are the standard deviation of measurements for bearing and range portions, respectively.

The birth process is modeled as an MB-RFS [4], which is given by $\pi_{\Gamma,k} = \{(r^{(i)}_{\Gamma,k}, p^{(i)}_{\Gamma,k}(x_k, s_k))\}^4_{i=1}$ where $r^{(1)}_{\Gamma,k} = r^{(2)}_{\Gamma,k} = 0.02$, $r^{(3)}_{\Gamma,k} = r^{(4)}_{\Gamma,k} = 0.03$, and $p^{(i)}_{\Gamma,k}(x_k, s_k) = t^{(i)}_{\Gamma,k}(s_k)\mathcal{N}(x_k; m^{(i)}_{\Gamma,k}(s_k), P^{(i)}_{\Gamma,k}(s_k))$, where $t^{(i)}_{\Gamma,k}(s_k) = [0.5, 0.5]$, $m^{(1)}_{\Gamma,k}(s_k) = [-1200, 0, 400, 0, 0]^T$, $m^{(2)}_{\Gamma,k}(s_k) = [-200, 0, 1050, 0, 0]^T$, $m^{(3)}_{\Gamma,k}(s_k) = [300, 0, 800, 0, 0]^T$, $m^{(4)}_{\Gamma,k}(s_k) = [800, 0, 1600, 0, 0]^T$, and $P^{(i)}_{\Gamma,k}(s_k) = \mathrm{diag}\{30, 30, 30, 30, 3 \times (\pi/180)\}^2$.

The survival probability is $p_{S,k} = 0.99$. The detection probability is $p_{D,k} = 0.98$. Clutter is modeled as a Poisson RFS with intensity [6]

$$\kappa_k = \lambda_c V u(z_k), \tag{69}$$

where λ_c is the average clutter intensity, V is the volume of the surveillance region, and $u(\cdot)$ is the uniform density over the surveillance region. The clutter density is set to $\lambda_c = 1.6 \times 10^{-3}(\text{rad m})^{-1}$ (an average of 10 clutter measurements per scan).

In the implementation of SUK-GM-MM-MB and UK-GM-MM-MB filters for nonlinear models, pruning and merging strategies are used to limit the number of hypothesized tracks and GM components [4],[6], each hypothesized track is pruned with a threshold of 10^{-4}, and the maximum of hypothesized tracks is 100. The pruning and merging threshold for GM components are 10^{-5} and 4, respectively. The maximum number of Gaussian components for each hypothesized track is 100. The scaling parameters for unscented transform are set to $\alpha = 1$, $\beta = 0$, and $\lambda = 2$.

In this numerical example, we compare the UK-GM-MM-MB and SUK-GM-MM-MB filtering approaches with the existing SMC-MM-MB filter for nonlinear models. In the implementation of the SMC-MM-MB filters, pruning of hypothesized tracks is performed with a threshold of 10^{-4}, too. To compare the filtering performance of the SMC-MM-MB filtering approach under different number of particles, two kinds of particles are used. SMC-MM-MB1: a maximum of $L_{\max} = 10000$ and a minimum of $L_{\min} = 3000$ particles is imposed for each hypothesized track; SMC-MM-MB2: a maximum of $L_{\max} = 5000$ and a minimum of $L_{\min} = 1000$ particles is imposed for each hypothesized track.

B. Metrics for Multi-Target Filtering

The optimal sub-pattern assignment (OSPA) metric [19] is considered for evaluating the filtering performance, since it can jointly capture difference in cardinality and individual elements between two finite sets. For two arbitrary finite sets $X = \{x_1, \cdots, x_m\}$ and $Y = \{y_1, \cdots, y_n\}$, the OSPA metric is defined as follows.

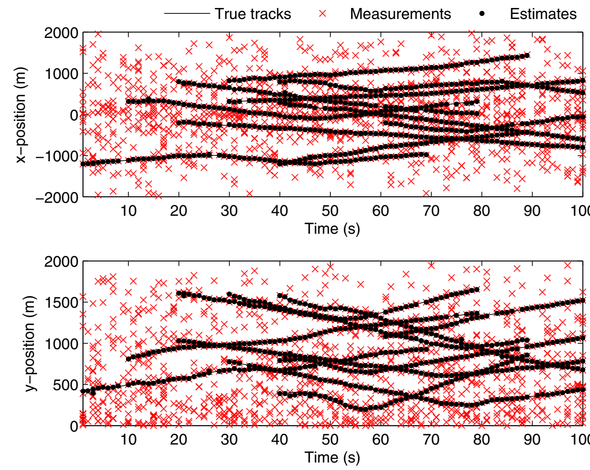

Fig. 2. True tracks, measurements, and estimates in xy positions versus time for the SUK-GM-MM-MB filtering approach.

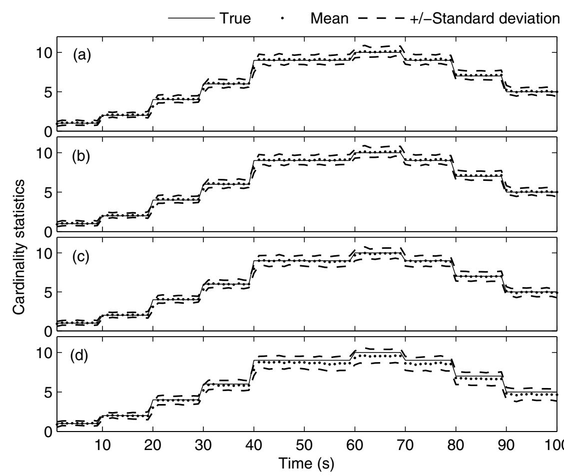

Fig. 3. Cardinality statistics versus time for (a) SUK-GM-MM-MB (b) UK-GM-MM-MB (c) SMC-MM-MB1 (d) SMC-MM-MB2.

$$\bar{d}^{(c)}_p(X, Y) := \begin{cases} \left(\frac{1}{n}\left(\min_{\pi\in\Pi_n} \sum_{i=1}^{m} d^{(c)}(x_i, y_{\pi(i)})^p + c^p(n-m)\right)\right)^{\frac{1}{p}}, & m \le n \\ \bar{d}^{(c)}_p(Y, X), & m > n \\ 0, & m = n = 0 \end{cases} \tag{70}$$

where $d^{(c)}(x, y) := \min(c, \|x - y\|)$, $\|\cdot\|$ is the Euclidean norm, and Π_n denotes the set of permutations on $\{1, 2, \cdots, n\}$. The OSPA metric can be decomposed into two components each separately accounting for localization and cardinality errors [19]. For $p < \infty$, the localization and cardinality errors

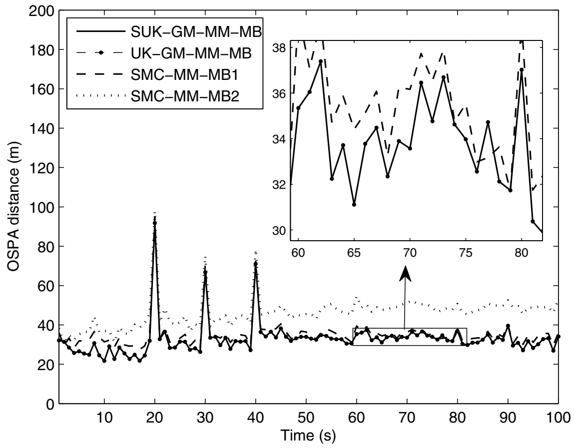

Fig. 4. The OSPA distance.

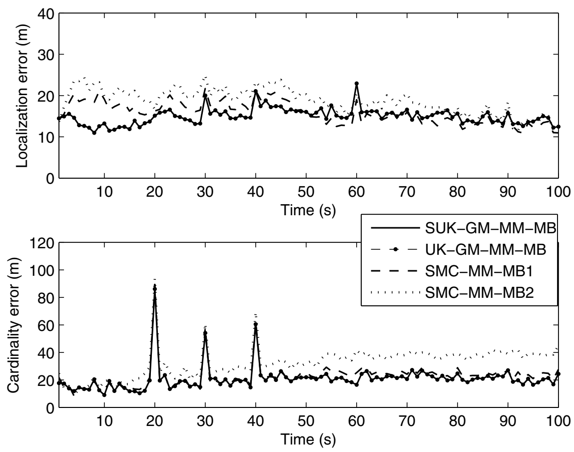

Fig. 5. Location and cardinality errors.

are given respectively by

$$\bar{e}^{(c)}_{p,loc}(X,Y) := \begin{cases} \left(\frac{1}{n}\left(\min_{\pi\in\Pi_n}\sum_{i=1}^{m} d^{(c)}(x_i, y_{\pi(i)})^p\right)\right)^{\frac{1}{p}}, & m \le n \\ \bar{e}^{(c)}_{p,loc}(Y,X), & m > n \end{cases} \tag{71}$$

$$\bar{e}^{(c)}_{p,card}(X,Y) = \begin{cases} \left(\frac{c^p(n-m)}{n}\right)^{\frac{1}{p}}, & m \le n \\ \bar{e}^{(c)}_{p,card}(Y,X), & m > n \end{cases} \tag{72}$$

The order parameter p determines the sensitivity to outliers, and the cut-off parameter c determines the relative weighting of the penalties assigned to cardinality and localization errors, for more details see [19]. In this paper, the parameters are set to $p = 2$ and $c = 200$.

TABLE I
COMPARISON OF THE FILTERING ACCURACY

Algorithm	Time avg. OSPA (m)	Time avg. loc. error (m)	Time avg. card. error (m)
SUK-GM-MB	32.7526	14.9246	20.8781
UK-GM-MB	32.7526	14.9246	20.8781
SMC-MB1	35.3897	15.8299	22.8230
SMC-MB2	46.1154	18.6798	32.4827

C. Monte Carlo Runs

To compare the filtering performance of these approaches for nonlinear models, 200 Monte Carlo (MC) runs are performed. In each MC simulation, the target trajectories are the same, but measurements are independently generated. Fig. 2 plots true tracks, measurements, and estimates in xy positions versus time for the SUK-GM-MM-MB filtering approach. It is shown that the SUK-GM-MM-MB is able to estimate multiple maneuvering targets' states. Fig. 3 plots the cardinality statistics. It is shown that the averages of the cardinality statistics of the SUK-GM-MM-MB, UK-GM-MM-MB and SMC-MM-MB1 converges to the true value, and the SMC-MM-MB2 deviates from the true value. The OSPA distance is plotted in Fig. 4. As shown in Fig. 4, the curves of the SUK-GM-MM-MB and UK-GM-MM-MB are indistinguishable, the filtering accuracy of SUK-GM-MM-MB and UK-GM-MM-MB is slightly better than that of SMC-MM-MB1, and the filtering accuracy of the SMC-MM-MB2 is the worst. The localization and cardinality errors are plotted in Fig. 5. From Fig. 5, the SUK-GM-MM-MB, UK-GM-MM-MB, and SMC-MM-MB1 show almost the same filtering performance in both localization and cardinality errors, and the filtering accuracy of the SMC-MM-MB2 is the worst in both localization and cardinality errors.

Table I gives the comparison of the filtering accuracy for these approaches. From Table I we can see that the SUK-GM-MM-MB shows exactly the same filtering accuracy as the UK-GM-MB in the time-averaged OSPA distance, localization and cardinality errors. The filtering accuracy of the SMC-MM-MB depends on the number of particles. The filtering accuracy is reduced when the number of particles is not enough. With the increasement of the number of particles, the filtering accuracy is improved. However, a large number of particles means a large amount of calculation. This will limit the realtime performance of the filtering approach. Overall, the SUK-GM-MM-MB and UK-GM-MM-MB filtering approaches are attractive approaches for nonlinear models.

Remark: For highly nonlinear models, the SMC-MM-MB filter is an attractive approach. For example, in track-before-detect (TBD) tracking, the measurement modes are highly nonlinear, the SMC implementation is a good choice. Note that the MCMC move step [20] can be applied to the SMC-MM-MB filter to increase the particle diversity. In addition, to reduce the number of particles, non-point particles, such as box particles [21] can also be considered for the SMC-MM-MB filter. However, these may be outside the scope of this paper.

V. Conclusion

In this paper, we propose the UK-GM implementation of the MM-MB filter for nonlinear models. In order to improve the robustness and numerical stability of the UK-GM-MM-MB filtering approach, the SUK-GM implementation of the MM-MB filter is presented. Simulation results demonstrate that the proposed approaches are able to estimate multiple maneuvering targets for nonlinear models, and SUK-GM-MM-MB and UK-GM-MM-MB produce the identical estimates. Recently, the labeled random finite set approaches [22],[23],[24] have been proposed to improve the estimating accuracy, which can also estimate targets' tracks. Extension of labeled random finite set approaches to MM will be considered in future work.

Acknowledgment

This work was supported in part by the National Natural Science Foundation of China under Grants 61222310, 61174142, and 61374021, the Zhejiang Provincial Natural Science Foundation of China under Grants LZ14F030002 and LZ14F030003, the Specialized Research Fund for the Doctoral Program of Higher Education of China (SRFDP) under Grants 20120101110115 and 20130101110109, the Open Fund for the Aircraft Marine Measurement and Control Joint Laboratory under Grant FOM2015OF009, the ASFC under Grant 20132076002, and the Fundamental Research Funds for the Central Universities under Grant 2014XZZX003-12.

References

[1] R. Mahler, "Multitarget Bayes filtering via first-order multitarget moments," *IEEE Trans. Aerosp. Electron. Syst.*, vol. 39, no. 4, pp. 1152–1178, Oct. 2003.

[2] ——, *Statistical Multisource-Multitarget Information Fusion*. Norwood: Artech House, 2007.

[3] ——, "PHD filters of higher order in target number," *IEEE Trans. Aerosp. Electron. Syst.*, vol. 43, no. 4, pp. 1523–1543, Oct. 2007.

[4] B.-T. Vo, B.-N. Vo, and A. Cantoni, "The cardinality balanced multi-target multi-Bernoulli filter and its implementations," *IEEE Trans. Signal Process.*, vol. 57, no. 2, pp. 409–423, Feb. 2009.

[5] B.-N. Vo, S. Singh, and A. Doucet, "Sequential Monte Carlo methods for multi-target filtering with random finite sets," *IEEE Trans. Aerosp. Electron. Syst.*, vol. 41, no. 4, pp. 1224–1245, Oct. 2005.

[6] B.-N. Vo, and W. Ma, "The Gaussian mixture probability hypothesis density filter," *IEEE Trans. Signal Process.*, vol. 54, no. 11, pp. 1091–4004, Nov. 2006.

[7] B.-T. Vo, B.-N. Vo, and A. Cantoni, "Analytic implementations of the cardinalized probability hypothesis density filter," *IEEE Trans. Signal Process.*, vol. 55, no. 7, pp. 3553–3567, Jul. 2007.

[8] B.-T. Vo, "Random finite sets in multi-object filtering," Ph.D. dissertation, The University of Western Australia, Perth,Australia, Oct. 2008.

[9] Y. Bar-Shalom, X.-R. Li, and T. Kirubarajan, *Estimation with Applications to Tracking and Navigation*. New York: Wiley, 2001.

[10] D. Dunne and T. Kirubarajan, "Multiple model multi-Bernoulli filters for manoeuvering targets," *IEEE Trans. Aerosp. Electron. Syst.*, vol. 49, no. 4, pp. 2679–2692, Oct. 2013.

[11] X. H. Yuan, F. Lian, and C. Z. Han, "Multiple model cardinality balanced multi-target multi-Bernoulli filter for tracking manoeuvering targets," *J. Appl. Math.*, vol. 2013, no. 727430, 2013.

[12] S. Blackman and R. Popoli, *Design and Analysis of Modern Tracking Systems*. Norwood: Artech House, 1999.

[13] S. Mcginnity and G. W. Irwin, "Multiple model bootstrap filter for maneuvering target tracking," *IEEE Trans. Aerosp. Electron. Syst.*, vol. 36, no. 3, pp. 1006–1012, Jul. 2000.

[14] J. Simon, and J. Uhlmann, "Unscented filtering and nonlinear estimation," *Proc. IEEE*, vol. 92, no. 3, pp. 401–422, Mar. 2004.

[15] S. Sarkka, *Bayesian Filtering and Smoothing*. Cambridge University Press, 2013.

[16] R. Van Der Merwe and E. A. Wan, "The square-root unscented kalman filter for state and parameter-estimation," in *IEEE Int. Conf. Acoust Speech Signal Process. Proc.*, Salt Lake, UT, United states, May 7-11, 2001, pp. 3461–3464.

[17] I. Arasaratnam and S. Haykin, "Cubature Kalman filters," *IEEE Trans. Automat. Control*, vol. 54, no. 6, pp. 1254–1269, Jun. 2009.

[18] Y. Bar-Shalom, P.K. Willett, and X. Tian, *Tracking and Data Fusion: A Handbook of Algorithms*. USA: YBS, 2011.

[19] D. Schuhmacher, B.-T. Vo, and B.-N. Vo, "A consistent metric for performance evaluation of multi-object filters," *IEEE Trans. Signal Process.*, vol. 56, no. 8, pp. 3447–3457, Aug. 2008.

[20] C. P. Robert and G. Casella, *Monte Carlo Statistical Methods*. New York: Springer, 2004.

[21] A. Gning, B. Ristic, L. Mihaylova, and F. Abdallah, "An introduction to box particle filtering," *IEEE Signal Process. Mag.*, vol. 30, no. 4, pp. 166–171, Jul. 2013.

[22] B.-T. Vo and B.-N. Vo, "Labeled random finite sets and multi-object conjugate priors," *IEEE Trans. Signal Process.*, vol. 61, no. 13, pp. 3460–3475, Jul. 2013.

[23] S. Reuter, B.-T. Vo, B.-N. Vo, and K. Dietmayer, "The labeled multi-Bernoulli filter," *IEEE Trans. Signal Process.*, vol. 62, no. 12, pp. 3246–3260, Jun. 2014.

[24] B.-N. Vo,B.-T. Vo, and D. Phung, "Labeled random finite sets and the Bayes multi-target tracking filter," *IEEE Trans. Signal Process.*, vol. 62, no. 24, pp. 6554–6567, Dec. 2014.